Rock Mech. Rock Engng. (2008) 41 (4), 563–585
DOI 10.1007/s00603-006-0124-5
Printed in The Netherlands

Rock Mechanics and Rock Engineering

Influence of Stochastic Discontinuity Network Parameters on the Formation of Removable Blocks in Rock Slopes

By

R. Jimenez-Rodriguez[1] and **N. Sitar**[2]

[1] ETS Ing. de Caminos, Canales y Puertos, Universidad Politécnica de Madrid, Spain; Formerly at Department of Civil and Environmental Engineering, University of California at Berkeley, USA
[2] Department of Civil and Environmental Engineering, University of California at Berkeley, USA

Received July 28, 2005; accepted September 14, 2006
Published online December 5, 2006

Summary

We study the effects of discontinuity network parameters on the formation of removable wedges in rock slopes. Discontinuities are simulated using the Poisson disk model, and removable wedges are identified using block theory. The formation of removable wedges of different sizes is assumed to follow a Poisson process. Poisson regression and Monte Carlo simulation are then used to identify statistically relevant parameters of the model, and to study the effects that variations in their values have on formation of removable blocks. The sensitivity of the results as a function of the mean orientations of the discontinuity sets forming the blocks is also studied by means of a parametric study. The volumetric intensity of discontinuities in the rock mass is found to have a significant impact on the computed estimates of removable block formation. As predicted by theory, our results indicate that, everything else being equal, the expected rate of formation of removable wedges is proportional to the square of the intensity measure. Estimates are also sensitive to changes in discontinuity size, especially in cases in which discontinuities are smaller than one to two times the height of the slope. The interaction between the mean size of discontinuities and the coefficient of variation of discontinuity sizes is found to be significant as well. Finally, results of our sensitivity analysis suggest that the orientation of discontinuity sets significantly affects the rate of formation of removable blocks in rock slopes.

Keywords: Block theory, fracture networks, Poisson disk model.

1. Introduction

Stochastic discontinuity network models are commonly employed to deal with uncertainties due to the stochastic nature of the geometry of rock masses and the variability of their mechanical properties (Dershowitz and Einstein, 1988; Lee et al., 1990; Meyer

and Einstein, 2002). Thus, being able to asses the influence that different parameters of the stochastic network model have on the engineering performance of the project of interest is a relevant aspect of rock engineering, as it allows one to optimize site characterization and design procedures, or at least to accomplish this more efficiently (Starzec and Andersson, 2002a).

In this work we address the problem of formation of removable blocks (i.e., blocks with kinematical admissibility for displacement toward the excavated free face) in excavations in "discontinuous" rock masses;[1] that is, rock masses intersected by planes of weakness, so that they are an assemblage of blocks closely fitted into a three dimensional arrangement (Goodman and Shi, 1985). Removability is a necessary condition for a block to fail, and keyblocks (i.e., blocks that are potentially critical for the stability of the excavation) are defined to be finite, removable, and unstable blocks (Goodman and Shi, 1985). Hence, predictions of the probability of removable block formation are needed when computing estimates of formation of keyblocks in rock excavations. To that end, once that removable blocks are identified, stability analyses may be performed to identify unstable blocks and to provide updated estimates of formation of keyblocks (see e.g., Dershowitz and Carvalho, 1996; Park and West, 2001; Starzec and Andersson, 2002b; Jimenez-Rodriguez and Sitar, 2003; Jimenez-Rodriguez, 2004; Park et al., 2005).

In this paper we study what are the main factors that may influence the formation of removable wedges (and therefore wedge failure). In particular, we study the effects of discontinuity network parameters on the formation of removable wedges in rock slopes. To that end, we use Monte Carlo simulation to generate successive realizations of the discontinuity network in the rock mass. Block theory (Goodman and Shi, 1985; Goodman, 1995) is then employed to identify removable blocks, and Poisson regression is used to develop a predictive model of the rate of formation of removable blocks of different sizes. Finally, we explore the significance that the governing parameters – or interactions between parameters – of the discontinuity network model have on the predicted rate of formation of removable blocks, identifying those that are (or are not) statistically relevant in the context of formation of removable blocks, and studying the effects of discontinuity network parameters on the formation of removable wedges.

2. Rock Mass Characterization and Slope Model

For the purpose of illustration of the methodology, we use discontinuity data from a road cut in a serpentine rock mass in southern Spain. The structure of the rock mass is characterized using discontinuity orientation data obtained by means of compass measurements of discontinuities selected using the scanline sampling method at exposed rock faces (Priest and Hudson, 1981; Priest, 1993). Scanlines with different orientations (along a horizontal line within the slope face; along the dip vector of the slope

[1] We use the general term *discontinuity* to refer to any mechanical break in the rock mass "having zero or low tensile strength" (ISRM, 1978). The term is therefore free from any connotation of geological origin, and is collectively used to refer to a wide variety of geological features, including weak bedding planes, tension cracks, joints, weakness zones and faults

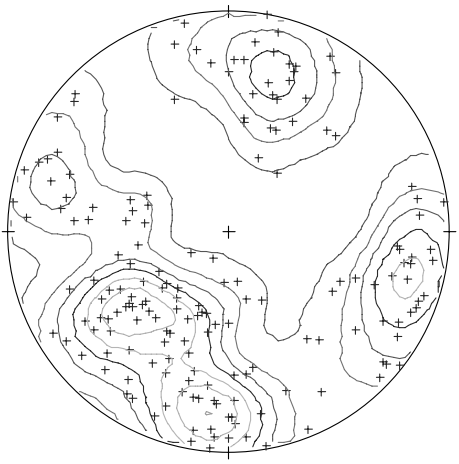

Fig. 1. Kamb's contours of lower hemisphere projections of poles of mapped discontinuities

face; and along a horizontal line in a plane approximately perpendicular to the slope face) are employed to reduce the effects of sampling bias, and five different joint sets are identified with the aid of program GEOPLOT (Ahlgren, 2000). Figure 1 shows an equal-angle, lower-hemisphere projection of the normal vectors of each discontinuity mapped, together with contour lines that represent the estimated frequency of discontinuity normals for each direction in space. The mean orientations (in the form of downward-pointing discontinuity normals and dip vectors; see Priest, 1993) of the five identified joint sets are listed in Table 1a.

In the analyses below, we consider a slope of height $H = 25\,\text{m}$ and width $W = 240\,\text{m}$, using the slope model shown in Fig. 2a. The orientations of the planar surfaces that form the top and face of the slope are listed (in strike-dip notation) in Table 1b. Joints existing within the rock mass are simulated using the Poisson disk

Table 1. Orientations of discontinuity sets and orientation of slope face and top

JS	Pole vector		Dip vector	
	Trend [deg]	Plunge [deg]	Trend [deg]	Plunge [deg]
(**a**) Mean orientations of joint sets considered				
1	231	33	051	57
2	103	10	283	80
3	186	11	006	79
4	016	16	196	74
5	285	10	105	80
		Strike [deg]		Dip [deg]
(**b**) Orientation of slope face and top				
Face		N216E		70NW
Top		N216E		20NW

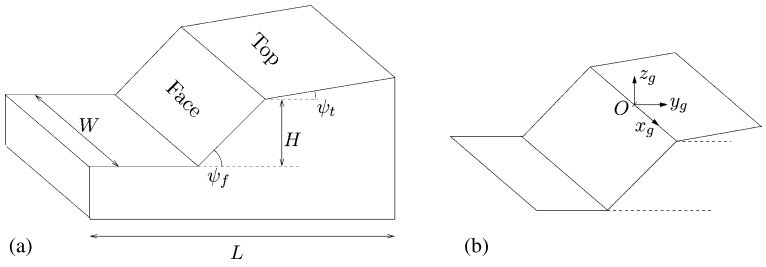

Fig. 2. Slope model considered, **a**) slope geometry; **b**) reference system for generation of discontinuity centers

model (Baecher et al., 1977; Dershowitz and Einstein, 1988; La Pointe, 1993). The Poisson disk model has been found to generate discontinuities that are often similar to natural discontinuity patterns and, in many cases, it has been recognized that discontinuity networks are best characterized by Poisson models (La Pointe, 1993; Bonnet et al., 2001). In other cases, however, discontinuity systems in rock masses are better described by power laws and fractal geometry (Bonnet et al., 2001; La Pointe, 2002), and fractals have also been widely used to describe the geometry of discontinuities (see e.g., Barton and Larsen, 1985; Boadu and Long, 1994; Kulatilake et al., 1997; Odling, 1997; Ehlen, 2000).

Following the Poisson disk model, discontinuity centers are assumed to be uniformly located within the generation domain – a rectangular parallelepiped whose sides are parallel to planes in the generation reference system shown in Fig. 2b. To reduce edge effects (see e.g., Chan and Goodman, 1987; Chan, 1987), the generation domain employed in the discontinuity simulation process has height $H_g = 400\,\text{m}$, width $W_g = 1000\,\text{m}$, and length $L_g = 800\,\text{m}$.

Discontinuities are further assumed to be circular, with their radius following a lognormal distribution with mean μ_R and coefficient of variation δ_R. The volumetric intensity $P_{32}[m^2/m^3]$ of generated discontinuities – defined as the ratio between area of discontinuities and rock volume (Dershowitz and Herda, 1992) – is another parameter of the discontinuity network, with discontinuities being generated until a threshold value of P_{32} is achieved. Finally, orientations of discontinuities in the rock mass are assumed to follow the Fisher distribution on the sphere, with discontinuity normals being generated around the mean pole orientation for each joint set in Table 1a, and with orientation variability defined by the concentration parameter, κ. To simulate orientations from the Fisher distribution, we use the method proposed by Fisher et al. (1981) as described in Fisher et al. (1987).

It should be clear that modeling assumptions listed above have limitations as compared to reality and that the influence of the variability of other parameters could be significant as well. For instance, Starzec and Andersson (2002a) studied the effect of orientation and termination mode on statistics of formation of keyblocks in underground excavations, concluding that changes in the orientation of discontinuities have a significant influence on keyblock predictions (in Section 5 we present a parametric study of the effects of discontinuity orientations on wedge removability), whereas the effect of changes in the termination fraction (i.e., the number of discontinuities that

terminate against other discontinuities over the total number of discontinuities) are not statistically significant. Therefore, conclusions developed in this study should not be applied to rock masses with a demonstrably different discontinuity system without due consideration to the errors that may be introduced.

3. Identification of Removable Wedges

Discontinuities within the rock mass can combine to form blocks of different shapes. Depending on the orientation of the excavation surface, some of these blocks will have the capability to move into the excavation – i.e., they are removable blocks. Goodman and Shi (1985) computed the number of different types of removable blocks that are theoretically formed by the combination of n joint sets, showing that it increases rapidly with n. Field studies based on observation of block moulds have shown, however, that most failed blocks actually belong to a subset of joint set combinations the failure likelihood of which is higher than the rest (Hatzor, 1992). Methods to compute the relative block failure likelihood of blocks formed by different joint set combinations have been proposed (Hatzor, 1993; Hatzor and Feintuch, 2005), and they can be used in the context of support design for rock excavations (Hatzor and Goodman, 1993).

These results allow designers to focus their characterization efforts only on joint sets forming blocks with high likelihood of failure, hence reducing the number of joint set combinations that need to be analyzed in practice. Visual observation of block moulds at our site suggested that the most significant joint sets were joint sets 1 and 3, and they are used for the analysis presented herein. Figure 3 shows examples of typical wedge moulds observed at the site.

In the context of computer simulations, we compute the intersections (if any) of each simulated joint with the planes that form the face and top of the slope (see Table 1b), using the formulation proposed by Chan (1987). Removable wedges in the excavation can then be identified using discontinuity traces formed by the inter-

Fig. 3. Examples of typical wedge moulds at the site

section of discontinuities with the excavation surface. To that end, we use block theory techniques (Shi et al., 1985; Shi and Goodman, 1989) on trace maps obtained after ''unrolling'' the top slope surface toward the slope face, and we follow Shi and Goodman's assumption that discontinuities extend far enough into the excavation so that trace loops obtained on the unrolled trace map delimit actual blocks. In the process of removable block identification, we take advantage of the peculiarities of our problem, as follows:

1. We assume that wedges are formed by discontinuities belonging to different joint sets. This is because discontinuities from the same joint set will form blocks with almost parallel faces, which are less likely to fail than blocks with faces that are not as close to being parallel (Hoek and Bray, 1981; Hatzor, 1993). In fact, it is customary to assume, as Shi and Goodman (1989) do, that blocks with parallel faces cannot move unless a non-dilatant shear behavior of the parallel faces is expected – e.g., they are smooth.
2. We only consider traces that intersect the line of intersection between the face and top of the slope (i.e., the hinge line employed in the ''unrolling'' operation), as discontinuity traces are required to intersect such hinge line to form a removable wedge.

Figure 4 shows an example of traces formed by the intersection of simulated discontinuities with the excavation surface. In addition, Fig. 4 illustrates the ''unrolling'' operation of discontinuity traces toward the face of the slope. Ellipses are the projected view of circular disks representing discontinuities. The disk on the left represents a discontinuity that does not intersect the excavated slope, whereas the disk on the right represents a discontinuity that intersects the excavation surface, producing two discontinuity traces. One such discontinuity trace (plotted with a discontinuous line) is ''unrolled'' toward the plane given by the slope face following the path indicated by the arrows. Similarly, Fig. 5a shows an example of the original (unrolled) map of all discontinuity traces that intersect the face and top of the slope; Fig. 5b (obtained after eliminating traces that do not intersect the hinge line between the face

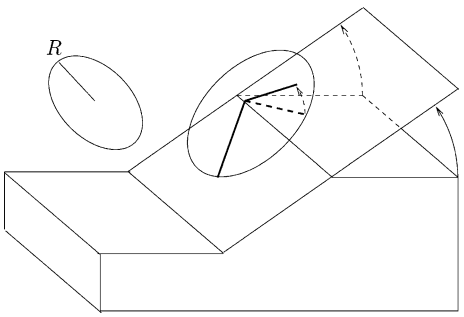

Fig. 4. Example of traces formed by the intersection of a simulated discontinuity with the excavation surface and graphical representation of the ''unrolling'' operation. The disk on the left represents a discontinuity that does not intersect the excavated slope. The disk on the right represents a discontinuity that intersects the excavation surface producing two discontinuity traces. The trace plotted with a discontinuous line is ''unrolled'' toward the slope face following the path indicated by the arrows

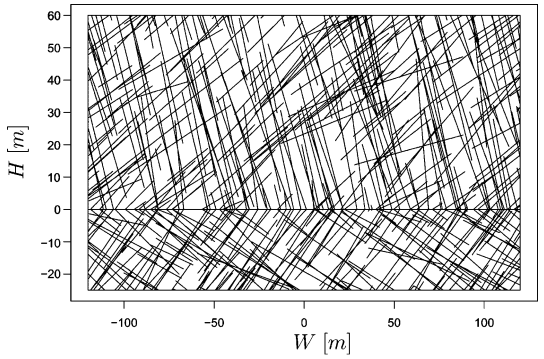

(a) Original unrolled trace map

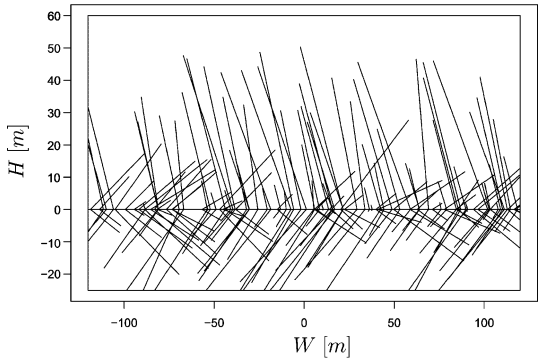

(b) Traces that may potentially form wedges

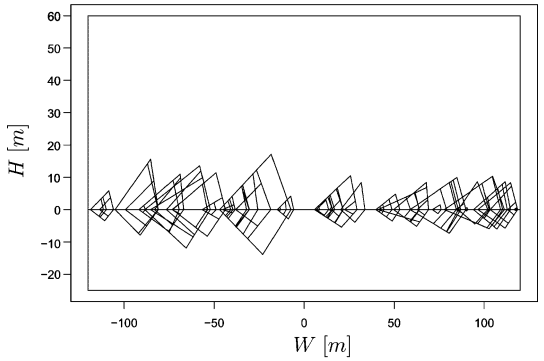

(c) Identified removable wedges

Fig. 5. Use of trace maps for the identification of removable blocks. Plots are made for a slope with height $H = 25\,\text{m}$ and orientation (in dip direction/dip format) 180/90 for its face and 180/00 for its top. Mean orientations for the two discontinuity sets considered are 155/40 and 245/40. Other parameters of the stochastic discontinuity network are $\mu_R = 30\,\text{m}$, $\delta_R = 0.8$, $P_{32} = 0.5\,\text{m}^{-1}$, and $\kappa = 200$

and top of the slope) shows those traces that may potentially form removable wedges; and, finally, Fig. 5c shows the removable wedges that were identified using block theory in that particular case.

Table 2. Nomenclature of size intervals considered for the analysis of identified removable wedges, with their corresponding interval limits

Interval names	I_1	I_2	I_3	I_4	I_5
Size limits	$[0, H/5]$	$[H/5, 2H/5]$	$[2H/5, 3H/5]$	$[3H/5, 4H/5]$	$[4H/5, H]$

It could be argued that, in general, the performance of the excavation will be worse as the number of removable and unstable blocks increases. However, the total number of removable blocks is known not to be a good indicator of the expected performance of an excavation, especially when small blocks that coalesce into larger blocks are not counted (McCullagh and Lang, 1984; Chan, 1987). This is because the total number of blocks does not provide information about the relative size of blocks that may eventually fail and, accordingly, it provides little information to estimate the consequences in the event of failure or to compute the necessary support measures. Having taken this issue into account, we consider wedge size in our analysis (defined as the vertical height of the wedge) and we record the number of removable wedges whose sizes are included within different size intervals. (Note that we count all identified removable blocks, even when such blocks are included within larger blocks or when they are formed as the intersection of larger blocks; see Fig. 5). As listed in Table 2, the five size intervals considered in this work range from $I_1 \equiv [0, H/5]$ to $I_5 \equiv [4H/5, H]$. That is, for instance, an identified removable wedge is recorded within size interval I_5 if the size of the wedge (i.e., its vertical height) is between 80 and 100% of the vertical height of the slope, H.

The potential number of removable and unstable blocks can also affect the mode of failure and the support needs of the excavation (see e.g., Karzulovic, 1988). For instance, field observations suggest that, as the number of blocks increases, the performance of the slope changes from structurally controlled rock block failures to a rubble-like failure mode of superficial small blocks or even to a mass failure mode similar to that commonly encountered in excavations in granular materials. However, to establish a relationship between the number of identified removable blocks within each size interval and the performance of the excavation is a challenging task beyond the scope of this paper, and we do not further discuss performance measures herein.

4. Statistical Analysis

Given the Poisson disk model used for generation of discontinuities, the formation of removable blocks along the excavation is expected to follow a Poisson process as well (see Ambartzumian et al., 1996, for an analytical derivation of this result). Accordingly, Poisson regression appears as a logical methodology to estimate the rate of formation of removable wedges of different sizes.

Poisson regression consists in estimating (via maximum likelihood) the dependance of the canonical parameter of the Poisson distribution, θ, on the input variables of the model (see Appendix A for details). The canonical parameter of the Poisson distribution is related to the rate of formation of removable wedges of different sizes, λ.

Table 3. Factors and levels considered in the Poisson regression analysis

Factor	Levels					
	−3	−2	−1	1	2	3
μ_R/H	1/3	2/3	1.0	1.5	2.0	4.0
δ_R		0.10	0.30	0.70	1.0	
$P_{32}\,[m^{-1}]$	0.4	0.7	1.0	1.5	3.0	5.0
κ		10.0	30.0	80.0	200.0	

Accordingly, once that the maximum likelihood estimates of the canonical parameter are computed for each size interval considered, $\hat{\theta}_i$, we may obtain estimates of the rate of formation of removable blocks within such size intervals, $\hat{\lambda}_i$. That is, as shown in Appendix A, we obtain $\hat{\lambda}_i$ as $\hat{\lambda}_i(\cdot) = \exp\hat{\theta}_i(\cdot)$, with $i = 1, \ldots, 5$.

4.1 Experimental Design and Regression Model

We consider four explanatory variables (i.e., factors) in the regression analysis, corresponding to rock discontinuity network parameters μ_R, δ_R, P_{32}, and κ. (As indicated in Section 2, μ_R is the mean radius of disks representing discontinuities, δ_R is the coefficient of variation of their radius, P_{32} is the intensity of discontinuities, and κ is the Fisher constant representing variability of discontinuity orientations around the mean orientation of the discontinuity set.) For each factor, we consider the values (i.e., levels) presented in Table 3. (Note that there are empty cells in Table 3 because a different number of levels is considered for each factor.)

A complete factorial design is employed, in which all combinations of factors and levels are considered, with a total of $d = 6^2 \cdot 4^2 = 576$ design points. (For the sake of simplicity, we assume that μ_R, δ_R, P_{32}, and κ are identical for both discontinuity sets in each design considered.) In addition, a series of twenty Monte Carlo simulations are performed for each design considered. In each case, a three dimensional discontinuity network is generated with the model presented in Section 2. For each generated network, traces produced by the intersection of discontinuities with the excavation surface are obtained; such traces are then employed (after performing the "unrolling" operation discussed in Section 3) to identify removable blocks of different sizes. Accordingly, the total experiment consists of $576 \cdot 20 = 11,520$ repetitions of the problem of generation of discontinuities and identification of removable wedges.

The following transformation of variables is performed for mathematical convenience prior to the regression analysis: $x_1 = \log(\mu_R/1.5H)$, $x_2 = \log(\delta_R/0.7)$, $x_3 = \log(P_{32}/1.5)$, and $x_4 = \log(\kappa/80)$. Accordingly, the vector of explanatory variables in the regression model is given by $\mathbf{x} \in \mathcal{X}$, where $\mathbf{x}$ represents the *transformed* parameter values of the discontinuity network model (i.e., $\mathbf{x} \equiv \{x_1, x_2, x_3, x_4\}$), and $\mathcal{X}$ indicates the design set in the Monte Carlo simulations performed (see Table 3).

In the analyses below, we focus on the formation of *medium* and *large*-sized removable blocks (i.e., within intervals $I_3 \equiv [2H/5, 3H/5]$ and $I_5 \equiv [4H/5, H]$). As explained in Appendix A, in both cases we consider an initial cubic model with a linear intercept, and statistically non-significant terms are eliminated iteratively in

Table 4. Maximum likelihood estimates of the coefficients of the medium-size and large-size removable blocks regression model

Term	Medium-sized			Large-sized		
	Estimate	Std. error	*P*-value	Estimate	Std. error	*P*-value
(Intercept)	−0.4356846	0.0025447	<2e-16	−1.022112	0.003425	<2e-16
x_1	0.5584750	0.0032470	<2e-16	1.212338	0.005182	<2e-16
x_2	0.2708231	0.0030892	<2e-16	0.777367	0.003884	<2e-16
x_3	1.9831220	0.0033840	<2e-16	1.982431	0.004434	<2e-16
x_4	0.0566357	0.0014392	<2e-16	0.154628	0.001932	<2e-16
x_1^2	−0.4788736	0.0029703	<2e-16	−0.763702	0.004697	<2e-16
x_2^2	−0.2539097	0.0057563	<2e-16	−0.324752	0.007761	<2e-16
x_3^2	0.0032999	0.0028752	0.25109	-0.012298	0.003738	0.00100
x_4^2	−0.0547446	0.0015669	<2e-16	−0.072206	0.002143	<2e-16
x_1^3	0.0968685	0.0019760	<2e-16	0.068759	0.003419	<2e-16
x_2^3	−0.1519567	0.0024689	<2e-16	−0.232509	0.003420	<2e-16
x_3^3	0.0077312	0.0026140	0.00310	0.014902	0.003614	3.73e-05
x_4^3	0.0206861	0.0008538	<2e-16	0.012439	0.001181	<2e-16
x_1x_2	−1.0881560	0.0040419	<2e-16	−1.877237	0.006506	<2e-16
x_1x_3	0.0010028	0.0021736	0.64456	−0.001016	0.003457	0.76887
x_1x_4	−0.0944563	0.0013864	<2e-16	−0.095362	0.002030	<2e-16
x_2x_3	−0.0048953	0.0025603	0.05588	–	–	–
x_2x_4	−0.0909339	0.0019126	<2e-16	−0.098851	0.002768	<2e-16
$x_2x_1^2$	0.2379372	0.0019815	<2e-16	0.577149	0.004993	<2e-16
$x_3x_1^2$	0.0053741	0.0027229	0.04842	0.014100	0.004394	0.00133
$x_4x_1^2$	0.0112822	0.0012313	<2e-16	–	–	–
$x_1x_2^2$	−0.3181284	0.0019425	<2e-16	−0.408644	0.003328	<2e-16
$x_4x_2^2$	−0.0239558	0.0010458	<2e-16	−0.020387	0.001522	<2e-16
$x_2x_3^2$	0.0090602	0.0021670	2.90e-05	–	–	–
$x_1x_4^2$	−0.0064471	0.0009707	3.09e-11	−0.020250	0.001494	<2e-16
$x_2x_4^2$	−0.0055073	0.0007060	6.17e-15	−0.015616	0.001041	<2e-16
$x_1x_2x_3$	0.0082710	0.0026439	0.00176	0.012151	0.003047	6.68e-05
$x_1x_2x_4$	0.0287085	0.0012048	<2e-16	0.026194	0.001925	<2e-16

a hierarchical manner considering a test of size $\alpha = 0.05$. Results presented in this section are computed using the R environment for statistical computing (R Development Core Team, 2004).

4.2 Formation of Medium and Large-Sized Removable Blocks

Table 4 lists the computed maximum likelihood estimates of terms found to be statistically relevant in the cubic regression model considered for predicting the formation of medium-sized (i.e., within size interval $I_3 \equiv [2H/5, 3H/5]$) and large-sized (i.e., within size interval $I_5 \equiv [4H/5, H]$) removable wedges.

Similarly, Figs. 6 and 7 present the rates of formation of medium and large-sized removable blocks that are predicted with the model.[2] Points in Figs. 6

[2] In Fig. 6 we emphasize the dependance of $\hat{\lambda}_3$ to changes in the mean size of discontinuities (as indicated by μ_R/H), whereas in Fig. 7 we emphasize the dependance of $\hat{\lambda}_5$ to changes in the intensity parameter, P_{32}. When $\hat{\lambda}_5$ is plotted against discontinuity mean size and $\hat{\lambda}_3$ is plotted against intensity, the overall shape of the model prediction curves is similar to the shape of curves in Figs. 6 and 7 and, in the interest of brevity, they are not reproduced herein (see e.g., Jimenez-Rodriguez and Sitar, 2005)

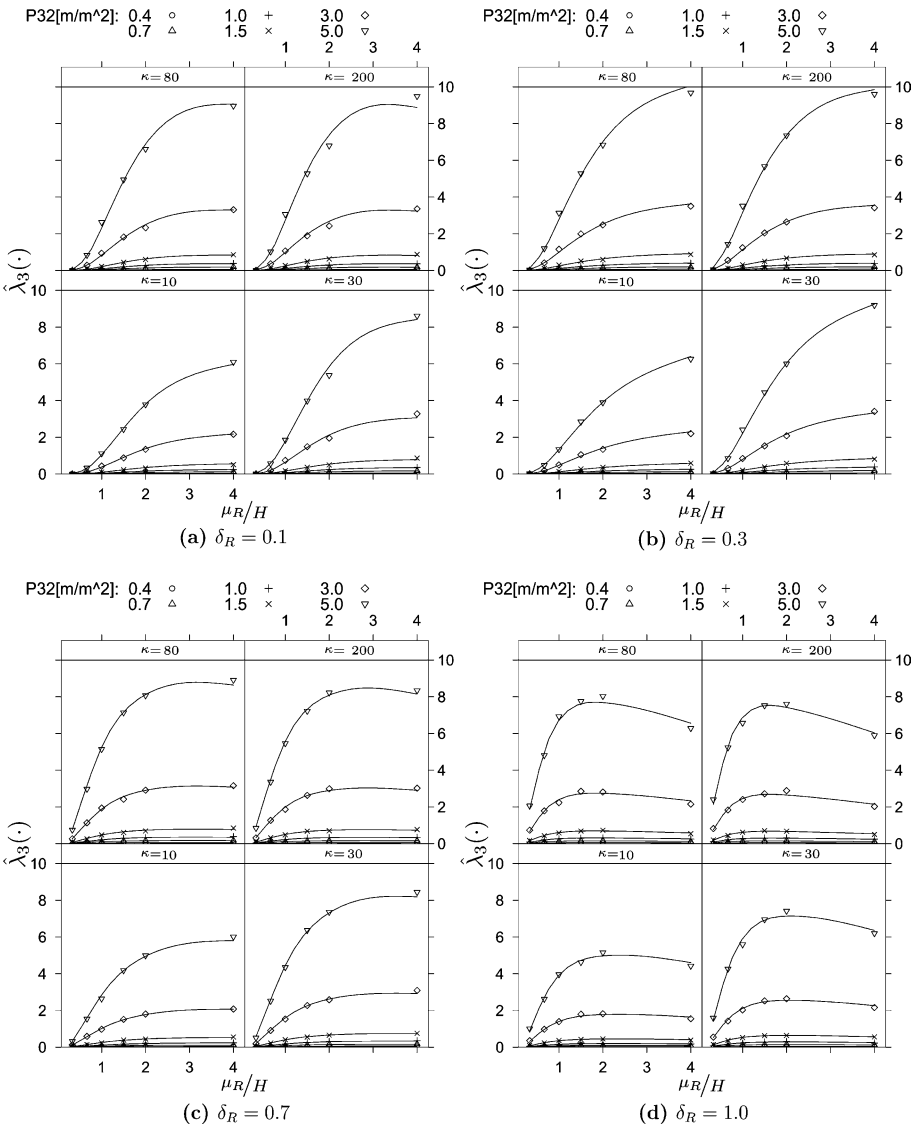

Fig. 6. Predicted rates of formation of medium-sized removable blocks as a function of the mean discontinuity radius, for different values of P_{32}, δ_R, and κ

and 7 indicate experimental data. That is, they indicate the mean rates of formation of removable wedges computed using the Monte Carlo simulations performed. Similarly, lines in Figs. 6 and 7 indicate predictions of the regression model. That is, given a set of values of the input parameters of the stochastic discontinuity network model, $\mathbf{x} \equiv \{x_1, x_2, x_3, x_4\}$, the lines indicate the mean rates of formation of removable wedges predicted by the model, as computed by $\hat{\lambda}_i(\mathbf{x}) = \exp\hat{\theta}_i(\mathbf{x})$.

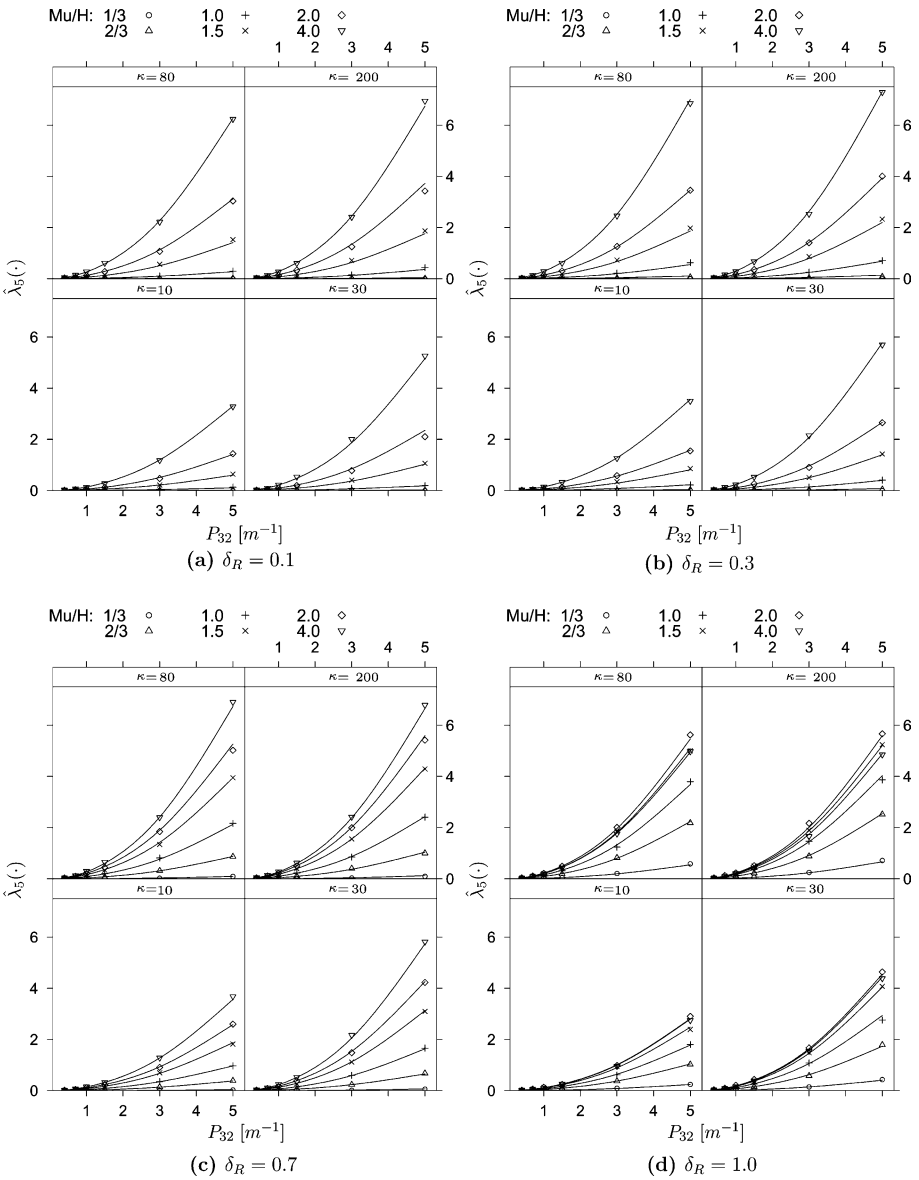

Fig. 7. Predicted rates of formation of large-sized removable blocks as a function of the intensity measure, for different values of μ_R/H, δ_R and κ

4.3 Discussion

Results show that, as expected in the context of the example case presented herein, the expected rate of formation of large removable blocks is somewhat smaller than the rate of formation of medium-sized blocks. This is mainly because, for discontinuities of a given size within the range considered herein (i.e., ‘‘not much larger’’ than the

slope size), a wider range of discontinuity locations will produce shorter traces yielding smaller blocks, as compared with the more restricted range of discontinuity locations that will yield longer traces and, therefore, larger blocks. Another reason is that large wedges can only be produced by the intersection of a fraction of the total sample of generated discontinuities; that is, small discontinuities cannot produce large wedges.

The effects of changes in the intensity of discontinuities can also be inferred from the computed simulations. Figures 6 and 7 show that increasing the volumetric intensity, P_{32}, significantly increases the rate of formation of medium and large-sized removable blocks ($\hat{\lambda}_3$ and $\hat{\lambda}_5$, respectively). In addition, our results show that these effects are independent of the value of the remaining input parameters (i.e., discontinuity sizes and variability of orientations) of the stochastic discontinuity network model. That is, interactions between intensity of discontinuities and other input parameters of the model are not significant in this particular case (e.g., see the low values of coefficients representing interaction between x_3 and other terms in Table 4).

Furthermore, our computed results of dependance of removable wedge formation on P_{32} agree well with the theoretical predictions. (Remember that the same value of P_{32} has been considered for both discontinuity sets.) In particular, if we consider the main effect of P_{32} only (see Table 4), the computed coefficient $\hat{\beta}_{x_3} \approx 1.98$ indicates that, everything else being equal, the expected rate of formation of medium and large-sized removable wedges is proportional to $(P_{32})^{1.98}$. Similarly, Mauldon (1992, 1994) (see also Hatzor and Feintuch, 2005) showed that, everything else being equal, increasing P_{32} of one set by a factor of K increases the probability of discontinuity intersections by the same factor, and increasing P_{32} of the other set by a factor of K increases it again by the same factor, therefore increasing the original intersection probability by a factor of K^2. Since joint intersection probabilities are related to probabilities of occurrence of rock blocks (Mauldon, 1994), the rate of formation of removable blocks within a given size interval is also increased by such factor. That is, the rate of formation of removable wedges is also proportional to $(P_{32})^2$, as our simulations indicate. Despite its importance, however, the intensity of discontinuities cannot be directly measured in general and it needs to be estimated using stereological principles and observations from area and line samples (Mauldon, 1994; see also Zhang and Einstein, 2000).

The mean size of discontinuities also affects the predictions of the model. This observation is to be expected since, as discussed above, the size of a wedge is bounded by the size of the smallest discontinuity forming the block. In this particular case, it is observed that the rate of formation of medium and large-sized removable blocks is particularly sensitive to changes in the size of discontinuities when discontinuities are smaller than approximately one to two times the height of the slope (i.e., $\mu_R/H < 2$). Conversely, predictions of formation of removable blocks are found to be less sensitive to changes in μ_R when larger discontinuities (i.e., with $\mu_R/H \geq 2$) are considered. (Note that curves plateau for high values of μ_R/H in Fig. 6.) In both cases, the sensitivity to changes in the normalized mean size of discontinuities, μ_R/H, is observed to depend on the variability of discontinuity sizes, as indicated by δ_R. In summary, the influence of the mean size of discontinuities on the formation of removable wedges depends on the variability of their sizes. (In statistical terminology, there is an interaction between μ_R/H and δ_R.) Such observation is further supported by the

high values of estimates for the coefficients of x_1x_2, $x_1x_2^2$, and $x_1^2x_2$ terms in Table 4. Information about the effects that interaction between input variables of the model have on the formation of removable wedges is not usually found in the literature on this topic, and it is an advantage of the proposed methodology (Starzec and Andersson, 2002a).

The results also show that increasing the concentration of discontinuity orientations toward the mean direction of each joint set has the effect of increasing the rate of formation of medium and large-sized removable wedges. In particular, when the variability of orientations is ''high'' (i.e., for ''low'' values of the concentration parameter, $\kappa < 30$), the predicted rates of formation of removable blocks are found to be significantly lower than in cases of ''low'' joint orientation variability (i.e., for ''high'' values of concentration parameter, with $\kappa > 30$). This observation, however, is not general and depends on the specific orientation of the discontinuity sets considered. For instance, given the requirement that two discontinuities must intersect to form a wedge, their highest probability of intersection occurs when the two sets have fixed orientations and they are perpendicular to each other (Mauldon, 1992, 1994; Hatzor and Feintuch, 2005). In that case, any variability in orientation will produce fewer intersections, since most pairs of generated discontinuities will not be orthogonal and will therefore have a reduced probability of intersection. On the other hand, if discontinuity sets are approximately parallel, then having variable orientation of the two sets will in general increase their probability of intersection and, therefore, the probability of removable wedge formation.

5. Effects of Mean Orientations of Discontinuities on Wedge Removability

In this section we perform a parametric study of the sensitivity of the results of removable wedge formation as a function of the mean orientations of the discontinuity sets forming the wedge. Such an analysis is performed to assess the influence of changes in the mean orientation of discontinuity sets on the formation of removable blocks of different sizes. To standardize the analysis, we consider a vertical slope face with E–W direction and a horizontal slope top. Similarly, we consider two discontinuity sets that intersect forming removable wedges within the slope. The orientations of such discontinuity sets are listed in Table 5. Empty cells appear in Table 5 because, for each discontinuity set, we have considered a different number of dip direction values (three) and dip values (two).

Table 5. Orientations of discontinuity sets considered in the analysis of sensitivity to mean orientation (α indicates dip direction values and β indicates dip values)

Orientation	Levels		
	−1	0	1
α_1	115	135	155
β_1	40		70
α_2	205	225	245
β_2	40		70

Table 6. Combinations of orientations of discontinuity sets considered in the analysis of sensitivity to mean orientation

Case	Levels			
	α_1	β_1	α_2	β_2
1	−1	−1	−1	−1
2	−1	−1	−1	1
3	−1	−1	0	−1
4	−1	−1	0	1
5	−1	−1	1	−1
6	−1	−1	1	1
7	−1	1	−1	−1
8	−1	1	−1	1
9	−1	1	0	−1
10	−1	1	0	1
11	−1	1	1	−1
12	−1	1	1	1
13	0	−1	−1	−1
14	0	−1	−1	1
15	0	−1	0	−1
16	0	−1	0	1
17	0	−1	1	−1
18	0	−1	1	1
19	0	1	−1	−1
20	0	1	−1	1
21	0	1	0	−1
22	0	1	0	1
23	0	1	1	−1
24	0	1	1	1
25	1	−1	−1	−1
26	1	−1	−1	1
27	1	−1	0	−1
28	1	−1	0	1
29	1	−1	1	−1
30	1	−1	1	1
31	1	1	−1	−1
32	1	1	−1	1
33	1	1	0	−1
34	1	1	0	1
35	1	1	1	−1
36	1	1	1	1

The different levels of discontinuity orientations (and their corresponding values) are combined into thirty-six cases. (The legend to denote the combinations of orientations that correspond to each case is presented in Table 6.) The height and width of the slope are considered identical as in the simulations discussed in Section 4, with values of $H = 25\,\text{m}$ and $W = 240\,\text{m}$. The remaining stochastic discontinuity network parameters considered during generation of discontinuities are $\mu_R = 1.4H$, $\delta_R = 0.4$, $P_{32} = 1.2\,\text{m}^{-1}$, and $\kappa = 200$. A series of ten Monte Carlo simulations are performed for each case listed in Table 6.

The numbers of identified removable wedges (after ten Monte Carlo simulations) within each size interval are listed in Table 7. The results corresponding to medium and large-sized removable wedges are also plotted in Fig. 8, and they indicate that the relative orientation of discontinuity sets has a significant influence on the number of

Table 7. Number of identified removable wedges for different combinations of orientations of the discontinuity sets forming the wedge (after ten Monte Carlo simulations; $H = 25\,\text{m}$, $\mu_R = 1.4H$, $\delta_R = 0.4$, $P_{32} = 1.2\,\text{m}^{-1}$, and $\kappa = 200$)

Case	Size interval				
	I_1	I_2	I_3	I_4	I_5
1	7607	2950	840	110	7
2	6396	3702	1918	899	300
3	9002	3733	1156	230	19
4	10226	5767	3073	1315	439
5	10264	3989	1000	151	9
6	11133	5850	2515	961	206
7	8996	3975	1435	417	67
8	5770	4045	2761	1775	1113
9	10201	5434	2629	1115	370
10	7535	5423	3826	2538	1532
11	11046	5688	2568	916	245
12	8448	5711	3772	2332	1357
13	5893	2128	609	101	7
14	6295	3544	1936	889	323
15	8440	3531	1268	357	50
16	9593	5560	2828	1255	485
17	10101	4153	1426	266	22
18	11308	6277	3139	1253	348
19	7419	3524	1514	518	117
20	5643	3962	2635	1705	1113
21	8649	4908	2671	1159	422
22	6426	4654	3196	2010	1306
23	9854	5665	2961	1380	461
24	7322	5336	3597	2423	1445
25	4809	1667	374	53	0
26	4783	2104	865	225	49
27	7031	2648	663	88	19
28	7670	3479	1301	364	91
29	7445	2653	663	105	4
30	9757	4578	1691	466	85
31	5196	2266	938	231	59
32	3498	2391	1590	1008	468
33	6533	3604	1793	807	278
34	5346	3672	2494	1537	893
35	6359	3856	2118	981	339
36	6452	4523	2917	1810	1084

identified removable wedges. Starzec and Andersson (2002a) obtained similar results and they also indicated that discontinuity orientation is a significant parameter influencing the formation of keyblocks. Similarly, the geometry of blocks has been identified as one key factor affecting the reliability of rock slopes with respect to stability considerations (see e.g., Jimenez-Rodriguez et al., 2006).

The results also show that the dip of the discontinuity sets appears as the most important factor affecting the formation of large removable wedges. Specifically, cases in which both discontinuity sets have high dip values (i.e., $\beta_1 = 70$ and $\beta_2 = 70$; corresponding to cases 8, 10, 12, 20, 22, 24, 32, 34, and 36) present the highest rate of formation of large-sized removable wedges whereas cases in which both discontinuity sets have low dip values (i.e., cases 1, 3, 5, 13, 15, 17, 25, 27, and 29) present the

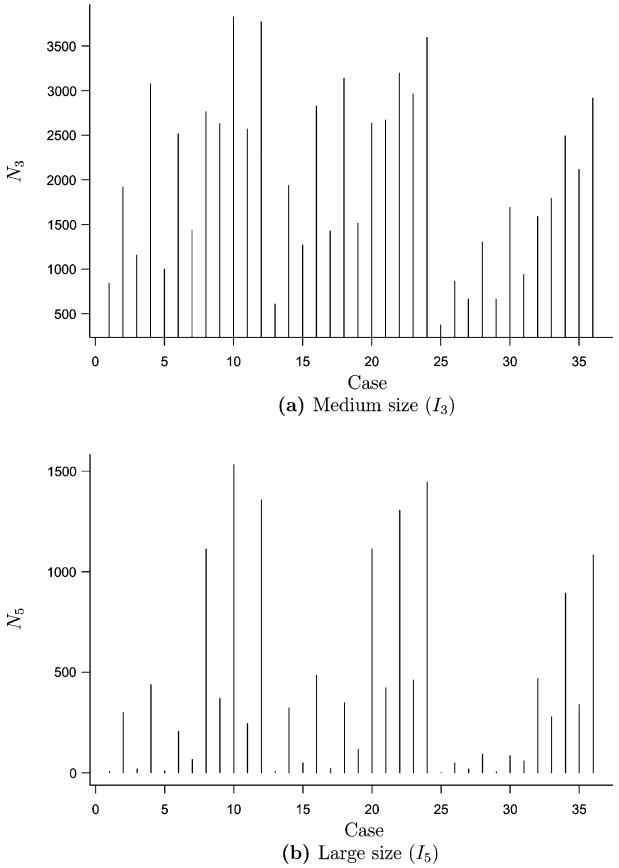

Fig. 8. Number of identified medium and large-sized removable wedges for different combinations of orientations of the discontinuity sets forming the wedge (after ten Monte Carlo simulations; $H = 25\,\text{m}$, $\mu_R = 1.4H$, $\delta_R = 0.4$, $P_{32} = 1.2\,\text{m}^{-1}$, and $\kappa = 200$)

lowest rate of formation of such wedges. (A similar observation can also be made for the case of medium-sized wedges, even though the effect is less significant than in the case of large-sized wedges.) The effect of ''aperture'' of the wedge (defined as the difference between the strikes of the discontinuity sets forming the wedge) is not, however, observed to be as important. In this sense, our results suggest that, in the context of formation of medium and large-sized ''centered'' removable wedges (i.e., they have dip directions symmetrical with respect to the dip direction of the slope), wedges with ''medium'' aperture (i.e., cases 15, 16, 21, and 22) tend to be slightly more likely than wedges with ''high'' aperture (i.e., cases 5, 6, 11, and 12). (Note that cases 22 and 12, however, seem to contradict this trend.) Similarly, wedges with ''high'' aperture are found to be somewhat more likely than wedges with ''low'' aperture (i.e., cases 25, 26, 31, and 32). The ''obliquity'' of the wedges with respect to the slope face is also found to affect the number of identified medium and large-sized removable blocks. In that sense, our results suggest that ''centered'' removable wedges (see e.g., cases 15, 16, 21, and 22) are slightly more likely than ''slanted''

wedges of the same aperture (cases 1, 2, 7, 8, 29, 30, 35, and 36). The influence of the ''obliquity'' of the wedges on their likelihood of formation, however, is also observed to be significantly smaller than the influence of the dip of the discontinuity sets.

6. Conclusions

We study the problem of evaluating the probability of formation of removable wedges in rock slopes. The Poisson disk model is used to generate (using Monte Carlo simulation) an extensive dataset of realizations of discontinuity networks. Traces formed by the intersection of discontinuities with the excavation surface are then used to identify removable wedges by means of block theory techniques. The formation of removable wedges is modeled as a Poisson process, and Poisson regression is used to develop a predictive model of the expected number of removable wedges of different sizes to be formed in the excavation.

In the context of the results presented in this work, we show that, as expected, the rate of formation of large-size removable blocks is significantly smaller than for medium-size blocks, and we also show that the overall trends of the predicted model responses are similar in both cases. In addition, we assess the influence that different parameters of the stochastic discontinuity network have on the estimated rate of formation of removable blocks. In particular, we show that:

- The volumetric intensity (P_{32}) of discontinuities in the rock mass has a significant impact on the estimates of removable block formation. As supported by theoretical considerations, our results suggest that, everything being equal, the expected rate of formation of removable wedges is proportional to the square of the intensity measure. In addition, interactions between intensity of discontinuities and other parameters of the discontinuity network model are not found to be relevant.
- The predictions of removable block formation are shown to be more sensitive to changes in the mean discontinuity radius, μ_R, when μ_R is ''small'' with respect to the height of the slope. Predictions of formation of removable blocks are also found to be less sensitive to changes in μ_R when larger discontinuities are considered. In addition, the influence of the mean size of discontinuities on the formation of removable blocks depends on the variability of their sizes. That is, in statistical terms, there is an interaction effect between the mean of the discontinuity radius distribution, μ_R, and its coefficient of variation, δ_R.
- The variability of discontinuity orientations with respect to the mean orientation of the joint set is found to have an influence on the formation of removable rock wedges. This observation, however, is not general and depends on the specific orientations of the discontinuity sets considered.

Furthermore, we show that variations of the mean orientation of discontinuity sets can have a significant influence on the number of identified removable wedges. The results also show that the dip of discontinuity sets appears as the main factor affecting the formation of removable wedges and, in particular, large removable wedges.

We can use these observations to make decisions for site characterization and engineering design in the context of the problem of keyblock formation. Given the significant influence that the intensity of discontinuities, P_{32}, has on the rate of for-

mation of removable blocks, we suggest that the adequate estimation of P_{32} should be a priority during site characterization for rock engineering. Despite its importance, however, the intensity of discontinuities cannot be directly measured and it needs to be inferred using stereological approaches.

The influence of the size of discontinuities within the rock mass is observed to depend on the relative size of discontinuities with respect to the excavation dimensions. In that sense, we should try to assure an accurate estimation of discontinuity sizes when discontinuities in the rock mass are smaller than approximately one to two times the slope dimensions; in case of larger discontinuities, however, our results suggest that an approximate estimation of discontinuity sizes could be acceptable, as the engineering consequences of such uncertainty do not appear significant.

Finally, results of our sensitivity analysis have shown that the adequate identification of discontinuity sets and characterization of their orientation should also be a priority during site characterization, as they have been found to significantly affect the formation of removable blocks.

Acknowledgments

Financial support for this research was provided by the Jane Lewis Fellowship from the University of California. The support of ''Grupo de Investigaciones Medioambientales: Riesgos Geológicos e Ingeniería del Terreno'' (RNM 221. PAI. Junta de Andalucía) of the University of Granada is also gratefully acknowledged. We would also like to thank two anonymous reviewers for their comments on an early version of the manuscript.

References

Ahlgren, S. (2000): GeoPlot: Plotting and Analysis Software for Microsoft Windows. http://www.geo.arizona.edu/coulomb/pages/geoplot/index.html.

Ambartzumian, R. V., DerKiureghian, A., Oganian, V. K., Sukiasian, H. S., Aramian, R. H. (1996): Poisson random planes model in tunnel building. Izvestiya Natsionalnoi Akademii Nauk Armenii. Matematika 31(2), 1–20.

Baecher, G. B., Einstein, H. H., Lanney, N. A. (1977): Statistical description of rock properties and sampling. In: Wang, F. D., Clark, G. B. (eds.), Energy resources and excavation technology; Proc., 18th U. S. Symp. on Rock Mech., Colo. Sch. Mines Press, Golden, pp. 5C1.1–5C1.8.

Barton, C., Larsen, E. (1985): Fractal geometry of two-dimensional fracture networks at Yucca Mountain, Southwestern Nevada. In: Stephansson, O. (ed.), Proc., Int. Symp. on Fundamentals of Rock Joints. Centek, Lulea, Sweden, pp. 77–84.

Boadu, F. K., Long, L. T. (1994): The fractal character of fracture spacing and rqd. Int. J. Rock Mech. Min. Sci. Geomech. Abst. 31(2), 127–134.

Bonnet, E., Bour, O., Odling, N., Davy, P., Main, I., Cowie, P., Berkowitz, B. (2001): Scaling of fracture systems in geological media. Rev. Geophys. 39(3), 347–383.

Chan, L.-Y. (1987): Application of block theory and simulation techniques to optimum design of rock excavations. PhD Thesis. University of California, Berkeley.

Chan, L.-Y., Goodman, R. E. (1987): Predicting the number of dimensions of key blocks of an excavation using block theory and joint statistics. In: Farmer, I. W., Daemen, J. J. K., Desai,

C. S., Glass, C. E., Neuman, S. P. (eds.), Rock mechanics; Proc., 28th U.S. Symp., A.A. Balkema, Rotterdam, pp. 81–87.

Dershowitz, W., Carvalho, J. (1996): Key-block tunnel stability analysis using realistic fracture patterns. In: Aubertin, M., Hassani, F., Mitri, H. S. (eds.), Proc., 2nd North American Rock Mechanics Symposium; NARMS '96, A Regional Conference of ISRM; Rock Mechanics Tools and Techniques, A. A. Balkema, Rotterdam, pp. 1747–1751.

Dershowitz, W. S., Einstein, H. H. (1988): Characterizing rock joint geometry with joint system models. Rock Mech. Rock Engng. 21(1), 21–51.

Dershowitz, W. S., Herda, H. H. (1992): Interpretation of fracture spacing and intensity. In: Tillerson, J. R., Wawersik, W. R. (eds.), Rock Mechanics; Proc., 33rd U.S. Symposium Rock Mechanics, A.A. Balkema, Rotterdam, pp. 757–766.

Dobson, A. J. (1990): An Introduction to Generalized Linear Models. Chapman & Hall, London.

Ehlen, J. (2000): Fractal analysis of joint patterns in granite. Int. J. Rock Mech. Min. Sci. 37(6), 909–922.

Fisher, N. I., Lewis, T., Embleton, B. J. J. (1987): Statistical analysis of spherical data. Cambridge University Press, Cambridge.

Fisher, N. I., Lewis, T., Willcox, M. E. (1981): Tests of Discordancy for Samples from Fisher's Distribution on the Sphere. Appl. Stat. 30(3), 230–237.

Goodman, R. E. (1995): Block theory and its application. Geotechnique 45(3), 383–422.

Goodman, R. E., Shi, G. (1985): Block theory and its application to rock engineering. Prentice-Hall international series in civil engineering and engineering mechanics. Prentice-Hall, Englewood Cliffs, N.J.

Hatzor, Y. (1992): Validation of block theory using field case histories. PhD Thesis. University of California, Berkeley.

Hatzor, Y. (1993): Block failure likelihood: a contribution to rock engineering in blocky rock masses. Int. J. Rock Mech. Min. Sci. Geomech. Abst. 30(7), 1591–1597.

Hatzor, Y., Feintuch, A. (2005): The joint intersection probability. Int. J. Rock Mech. Min. Sci. 42(4), 531–541.

Hatzor, Y., Goodman, R. E. (1993): Determination of the ''design block'' for tunnel supports in highly jointed rock. In: Fairhurst, C., Hudson, J. A. (eds.), Comprehensive rock engineering; principles, practice & projects, Pergamon Press, Oxford, pp. 263–292.

Hoek, E., Bray, J. (1981): Rock slope engineering. Institution of Mining and Metallurgy, London, rev. 3rd edn.

ISRM (1978): Suggested methods for the quantitative description of discontinuities in rock masses. Int. J. Rock Mech. Min. Sci. Geomech. Abst. 15(6), 319–368.

Jimenez-Rodriguez, R. (2004): Probabilistic identification of keyblocks in rock excavations. PhD Thesis. University of California, Berkeley.

Jimenez-Rodriguez, R., Sitar, N. (2003): Probabilistic identification of unstable blocks in rock excavations. In: der Kiureguian, A., Madanat, S., Pestana, J. (eds.), Application of Statistics and Probability in Civil Engineering. Millpress, Rotterdam, vol. 2, pp. 1301–1308.

Jimenez-Rodriguez, R., Sitar, N. (2005): Influence of stochastic discontinuity network parameters on the formation of removable blocks in rock slopes. GeoEngineering report, Department of Civil and Environmental Engineering, University of California, Berkeley. In press.

Jimenez-Rodriguez, R., Sitar, N., Chacón, J. (2006): System reliability approach to rock slope stability. Int. J. Rock Mech. Min. Sci. 43(6), 847–859.

Karzulovic, A. L. (1988): The use of keyblock theory in the design of linings and supports for tunnels. PhD Thesis. University of California, Berkeley.

Kulatilake, P., Fiedler, R., Panda, B. B. (1997): Box fractal dimension as a measure of statistical homogeneity of jointed rock masses. Engng. Geol. 48(3–4), 217–229.

La Pointe, P. R. (1993): Pattern analysis and simulation of joints for rock engineering. In: Hudson, J. A. (ed.), Comprehensive rock engineering, Pergamon Press, Oxford, vol. 3 – Rock testing and site characterization, pp. 215–239.

La Pointe, P. R. (2002): Derivation of parent fracture population statistics from trace length measurements of fractal fracture populations. Int. J. Rock Mech. Min. Scie. 39, 381–388.

Lee, J. S., Veneziano, D., Einstein, H. H. (1990): Hierarchical fracture trace model. In: Hustrulid, W. A., Johnson, G. A. (eds.), Rock mechanics; contributions and challenges; Proc., 31st U.S. Symposium, A.A. Balkema, Rotterdam, pp. 261–268.

Mauldon, M. (1992): Relative probabilities of joint intersections. In: Tillerson, J. R., Wawersik, W. R. (eds.), Rock mechanics; Proc., 33rd U.S. Symposium, A.A. Balkema, location varies, pp. 767–774.

Mauldon, M. (1994): Intersection probabilities of impersistent joints. Int. J. Rock Mech. Min. Sci. Geomech. Abst. 31(2), 107–115.

McCullagh, P., Lang, P. (1984): Stochastic models for rock instability in tunnels. J. Roy. Stat. Soc. B. Met. 46(2), 344–352.

McCullagh, P., Nelder, J. A. (1989): Generalized linear models. Chapman & Hall/CRC, Boca Raton, Florida, 2nd edn.

Meyer, T., Einstein, H. H. (2002): Geologic stochastic modeling and connectivity assessment of fracture systems in the Boston area. Rock Mech. Rock Engng. 35(1), 23–44.

Odling, N. (1997): Scaling and connectivity of joint systems in sandstones from western Norway. J. Struct. Geol. 19(10), 1257–1271.

Park, H., West, T. R. (2001): Development of a probabilistic approach for rock wedge stability. Engng. Geol. 59, 233–251.

Park, H.-J., West, T. R., Woo, I. (2005): Probabilistic analysis of rock slope stability and random properties of discontinuity parameters, Interstate Highway 40, Western North Carolina, USA. Engng. Geol. 79(3–4), 230–250.

Priest, S. D. (1993): The collection and analysis of discontinuity orientation data for engineering design, with examples. In: Hudson, J. A. (ed.), Comprehensive rock engineering; principles, practice & projects: Rock testing and site characterization, Pergamon Press, Oxford, pp. 167–192.

Priest, S. D., Hudson, J. A. (1981): Estimation of discontinuity spacing and trace length using scanline surveys. Int. J. Rock Mech. Min. Sci. Geomech. Abst. 18(3), 183–197.

R Development Core Team (2004): R: A language and environment for statistical computing. R Foundation for Statistical Computing, Vienna, Austria. URL http://www.R-project.org.

Shi, G.-H., Goodman, R. E. (1989): The key blocks of unrolled joint traces in developed maps of tunnel walls. Int. J. Numer. Anal. Met. Geomech. 13(2), 131–158.

Shi, G.-H., Goodman, R. E., Tinucci, J. P. (1985): Application of block theory to simulated joint trace maps. In: Stephansson, O. (ed.), Proc., Int. Symp. Fundamentals of Rock Joints, CENTEK Publ., Lulea, pp. 367–383.

Starzec, P., Andersson, J. (2002a): Application of two-level factorial design to sensitivity analysis of keyblock statistics from fracture geometry. Int. J. Rock Mech. Min. Sci. 39(2), 243–255.

Starzec, P., Andersson, J. (2002b): Probabilistic predictions regarding key blocks using stochastic discrete fracture networks – example from a rock cavern in south-east Sweden. Bulletin Engineering Geology and Environment 61(4), 363–378.

Stone, C. J. (1996): A course in probability and statistics. Duxbury Press, Belmont.

Venables, W. N., Ripley, B. D. (2002): Modern Applied Statistics with S. Fourth Edition. Statistics and Computing. Springer, New York.

Zhang, L. Y., Einstein, H. H. (2000): Estimating the intensity of rock discontinuities. Int. J. Rock Mech. Min. Sci. 37(5), 819–837.

A. Poisson Regression

The Poisson distribution is an example of distributions included within the one-parameter exponential family of statistical distributions. Within that context, the probability function of the Poisson distribution can be written as (Stone, 1996):

$$f(y;n,\theta) = e^{\theta y - nC(\theta)} r(y;n), \qquad y \in \mathscr{Y}_n \tag{1}$$

where $\mathscr{Y}_n = \{0, 1, 2, \ldots\}$ represents the possible outcomes of the number of identified removable wedges and n can be viewed as "units of exposure" relative to which the rate of the Poisson process is expressed (Dobson, 1990) – for instance, it corresponds to the lateral extension of the slope considered in the problem of removable block formation that we study herein. Additionally, the canonical parameter of the Poisson distribution, θ, is related to the rate of the Poisson process, λ, by the expression $\theta = \log\lambda$. We also have that $C(\theta) = e^{\theta}$ and $r(y;n) = n^y/y!$. It may be further observed that θ ranges over $(-\infty, +\infty)$ as λ ranges over $(0, +\infty)$.

To perform the regression analysis, following Stone (1996), we denote $\lambda(\cdot)$ as the rate function and $\theta(\cdot)$ as the canonical function. Therefore, the dependance of λ on the explanatory variables $\mathbf{x} \in \mathscr{X}$ is given by $\lambda(\mathbf{x})$, and the dependence of θ on $\mathbf{x} \in \mathscr{X}$ is given by $\theta(\mathbf{x})$, with $\mathscr{X}$ being the design set considered for the explanatory variables. It is generally preferred to perform the regression analysis over the canonical function rather than over the rate function, and this is the approach that we use in this work. To that end, it is assumed that $\theta(\cdot)$ belongs to an identifiable p-dimensional linear space G, with functions $\{g_1, \ldots, g_p\}$ forming a basis of G. Then, $\theta(\cdot) \in G$ may be expressed as a unique linear combination of the functions in the basis, in the form $\theta(\cdot) = \beta_1 g_1 + \cdots + \beta_p g_p$, and the rate function may be obtained by $\lambda(\cdot) = \exp(\beta_1 g_1 + \cdots + \beta_p g_p)$.

The problem of performing Poisson regression consists of finding the maximum likelihood estimators of the β_i coefficients, that will be referred to as $\hat{\beta}_i$, with $i = 1, \ldots, p$. Such values provide the model estimate that maximizes the likelihood of observing the available data under the assumption that $\theta(\cdot) \in G$.

In both regression analyses presented in this work we consider an initial cubic regression model. That is, the regression function $\theta(\cdot)$ is initially assumed to be included in a space, G, formed by the span of functions that are powers of up to order three of the transformed explanatory variables (i.e., terms such as x_i, x_i^2, and x_i^3) and their interactions, also up to power three (i.e., terms such as $x_i x_j$, $x_i^2 x_j$, $x_i x_j x_k$, etc.). A linear intercept (i.e., a constant term) is also included, which makes the total dimension of the regression model to be $p = 35$. The $p = 35$ dimension of the regression

space is divided as follows: one constant for the linear intercept, twelve main factor terms (i.e., four terms of type x_i, four of type x_i^2, and four of type x_i^3), six interaction terms of type $x_i x_j$, twelve interaction terms of type $x_i x_j^2$, and, finally, four interaction terms of type $x_i x_j x_k$.

The discussion above indicates that there are thirty-five regression coefficients, β_i, that need to be estimated to solve the regression problem. Explicit expressions to compute the maximum likelihood estimates of such coefficients, $\hat{\beta}_i$, are not usually available, and they need to be calculated iteratively. The iterative (re)weighted least-squares algorithm is commonly used for such tasks, involving the iterative solution of a series of linear systems, with the system coefficients changing from iteration to iteration (McCullagh and Nelder, 1989; Stone 1996; Venables and Ripley, 2002).

To perform model selection, statistically non-significant terms are eliminated iteratively in a hierarchical manner. That is, a term is removed only if no statistical evidence is found to reject the hypothesis that $\beta_i = 0$ and if the model includes no other terms which depend on higher order powers of variables included in such a term (e.g., the term $x_i x_j$ cannot be eliminated if $x_i x_j^2$ is still included in the model). To test the hypothesis that $\beta_i = 0$, we use the P-value of the test with the usual statistical interpretation; i.e., for the test of size α (the size of the test indicates the probability of erroneously rejecting a valid hypothesis) the hypothesis is rejected if α is greater or equal than the P-value, and it is not rejected if α is less than the P-value (Stone, 1996).

Finally, once that the statistically significant terms of the canonical function have been identified and the maximum likelihood estimates of their coefficients have been computed, we may use the relationship between the canonical function and the rate function of the Poisson distribution to obtain estimates of the rate of formation of removable blocks within each size interval considered, $\hat{\lambda}_i$. That is, given that $\theta_i = \log\lambda_i$, we obtain $\hat{\lambda}_i$ as $\hat{\lambda}_i(\cdot) = \exp\hat{\theta}_i(\cdot)$, with $i = 1, \ldots, 5$.

Author's address: Dr. Rafael Jimenez-Rodriguez, ETS Ing. de Caminos, Canales y Puertos. Universidad Politecnica de Madrid, Spain; e-mail: rjimenez@caminos.upm.es